Bioorganic Chemistry 104 (2020) 104302

Contents lists available at ScienceDirect

Bioorganic Chemistry

journal homepage: www.elsevier.com/locate/bioorg

Design, synthesis and evaluation of diaryl γ-dihydropyrone derivatives as cyclocurcumin mimetics and inhibitors of the aggregation of amyloid β

Mayumi Hotsumi, Misato Tajiri, Koki Makabe, Hiroyuki Konno *

Department of Biochemical Engineering, Graduate School of Science and Engineering, Yamagata University, Yonezawa, Yamagata 992-8510, Japan

ARTICLE INFO

Keywords:
Amyloid β
Cyclocurcumin
Diaryl γ-dihydropyrone
Water soluble
Amyloid β aggregation

ABSTRACT

A structure activity relationship study of cyclocurcumin-derived, diaryl γ-dihydropyrone-based inhibitors of amyloid β aggregation is described. Optimization of the diaryl γ-dihydropyrone framework and two phenolic rings resulted in the identification of diaryl γ-dihydropyrone type cyclocurcumin analogue AY1511, which exhibited potent anti-amyloid β aggregation activity (leading to nanorod-like fragments), sufficient water solubility, and low cytotoxicity.

1. Introduction

Amyloid β (Aβ) is a group of peptides consisting of 39–43 amino acid residues produced by the cleavage of amyloid β precursor protein in the cell membrane of neurons, aggregates of which accumulate in the brain and causes neuronal cell death and Alzheimer's disease [1]. Aβ(1–42) consisting of 42 amino acid residues is particularly prone to aggregate and therefore especially toxic, and one potential strategy for the treatment of Alzheimer's patients is the inhibition of this process (Fig. 1).

In previous work, we undertook a structure activity relationship study of derivatives of CUR (**1**), an acidic polyphenol incorporating unsaturated aliphatic and aromatic groups extracted from the rhizome of turmeric (*Curcuma longa*) [2]. Turmeric has been used as a spice, pigment and medicine in India for centuries, and CUR (**1**) is posited to have anti-inflammatory and anti-cancer effects [3–11], but its very poor water solubility and rapid metabolization after oral administration precludes clinical use [12–16]. We discovered the C5-curcuminoid (AY1319, **3**), which comprises two phenolic rings connected by C5-sp^2 carbons and was found to exhibit high Aβ aggregation inhibitory activity and sufficient water solubility [17–20]. However, curcuminoids incorporating sp^2 carbons are poorly water stable, and those based on more stable, rigid frameworks are needed. Cyclocurcumin (CYC, **2**) reported by Kiuchi et al is a minor curcuminoid formed by intramolecular Michael addition of CUR (**1**) and shown to have a synergistic effect with CUR (**1**) as a nematicide and inhibitor of the growth of human breast cancer MCF-7 cells [21–23]. Herein, we report our pursuit of water soluble diaryl γ-dihydropyrone type derivatives (**4**) with anti Aβ aggregation activity and stability by mimicking CYC (**2**).

2. Results and discussion

The first step was to design a framework to serve as the basis of a selection of derivatives. Although CYC (**2**), composed of a rigid carbon framework and sp^2 carbon spacer, is an attractive target due to its interesting biological activities, it is poorly stable in water and difficult to prepare. Accordingly, informed by our experience with C5-curcuminoid derivatives and a knowledge of their structure activity relationships, removal of olefin moiety of CYC (**2**) was performed to give the general diaryl γ-dihydropyrone-based framework (**4**), from which eleven synthetic targets (**7**–**9**) were designed including the mono aryl γ-dihydropyrones (**7a-b**), to optimize the number of aryl groups; compounds (**8a-c**), which bear methoxy groups at the 3-position of the phenyl rings as in CUR (**1**) and CYC (**2**); and diaryl γ-dihydropyrones (**9a-f**), wherein the hydroxy groups are in other positions. All eleven γ-dihydropyrone derivatives (**7a-b, 8a-c, 9a-f**) were synthesized using the Khera method [24].

Aldol reaction of the appropriate acetophenone and ethyl acetate in the presence of NaHMDS affords the diketone derivatives (**5**), which were treated with a variety of benzaldehydes (**6**) and either LDA or NaHMDS to give the corresponding hydroxy diketones. After HCl-promoted cyclization and dehydration, the requisite aryl γ-dihydropyrones (**7a-b, 8a-c, 9a-f**) were obtained. Schemes 1–3 present the benzaldehyde derivatives (**6a-g**) and the diketones (**5a-c**) that were used as coupling partners. The benzaldehydes (**6a-g**) and acetylacetone are

* Corresponding author.
E-mail address: konno@yz.yamagata-u.ac.jp (H. Konno).

https://doi.org/10.1016/j.bioorg.2020.104302
Received 12 June 2020; Received in revised form 27 August 2020; Accepted 18 September 2020
Available online 22 September 2020

commercially available; diketone derivatives (**5a-c**) were prepared by us as described in the supporting information.

Aryl γ-dihydropyrones (**7a-b**) were synthesized shown in Scheme 1. Aldol reaction of acetylacetone (**5a**) and benzaldehyde (**6a-b**) in the presence of base afforded 6-hydroxy-6-phenyl-hexane-2,4-dione derivatives. Treatment of the corresponding diones with 4 M HCl followed by cyclization and dehydration gave **7a** and **7b** in yields of 14% and 38%, respectively (Scheme 1).

Next, diaryl γ-dihydropyrones (**8a-c**) were prepared, Scheme 2. Though the synthetic protocol used was similar to that used to prepare the 6-hydroxy-6-phenyl-hexane-2,4-dione derivatives, protection of the hydroxy groups of the acetophenone (**5b**) was necessary for the Aldol reactions to proceed. In these cases, methoxyethoxymethyl (MEM) ether protecting group was selected. The desired diaryl γ-dihydropyrones (**8a-c**) were obtained after treatment with 4 M HCl (Scheme 2).

As depicted in Scheme 3, diaryl γ-dihydropyrones (**9a-f**) were synthesized. The diketone derivatives (**5c**) and the benzaldehydes (**6a-g**) were coupled to give diaryl γ-dihydropyrones (**9a-f**). Chemical yields of the desired γ-dihydropyrones (**7a-b, 8a-c, 9a-f**) ranged from 3 to 38% due to difficulties associated with the control of these transformation sequences (intermediates and by-products were isolated, though not characterized). Although chemical yields of γ-dihydropyrone formations were low, quantities of all target compounds sufficient for their evaluation were obtained, and their chemical structures were confirmed by ^{1}H- and ^{13}C NMR, IR, and MS spectroscopy (see experimental). The NMR spectra of all synthesized γ-dihydropyrone derivatives rings contained the expected characteristic peaks, including a singlet at 5.97 ppm corresponding to the α-methine proton of the olefin moiety, and doublet-doublet at 5.78 ppm corresponding to the β-methine proton of **9f.**

The "shake flask" method (see experimental) was used to evaluate the water solubility of the eleven synthesized γ-dihydropyrones (**7a-b, 8a-c, 9a-f**) compared to those of CUR (**1**), AY1031 and AY1319 (**2**) [25]. Identical molar quantities of both standard curcuminoids; CUR (**1**) and AY1319 (**2**) and the synthesized γ-dihydropyrones (**7a-b, 8a-c, 9a-f**) were vortexed in water, and the resulting solutions centrifuged to remove undissolved material. The supernatant liquid was concentrated and the residue re-dissolved in MeOH for analysis by RP-HPLC. The results are summarized in Table 1. Using this assay, the water solubility of CUR (**1**) was calculated to be 0.19 μM, and that of AY1319 (**2**) was 271 μM. The water solubilities of all the synthesized γ-dihydropyrones (**7a-b, 8a-c, 9a-f**) were higher both CUR (**1**) and AY1031 [21]. Thus, compounds based on the γ-dihydropyrone framework were confirmed to be more water soluble compared with derivatives of C7-curcuminoid. A particularly dramatic improvement in water solubility was observed for monoaryl γ-dihydropyrones **7a** and **7b** (bearing one aromatic ring). The water solubility of **7b** was the highest of the derivatives synthesized, 15,520 times higher than that of CUR (**1**), and 11.5 times than that of

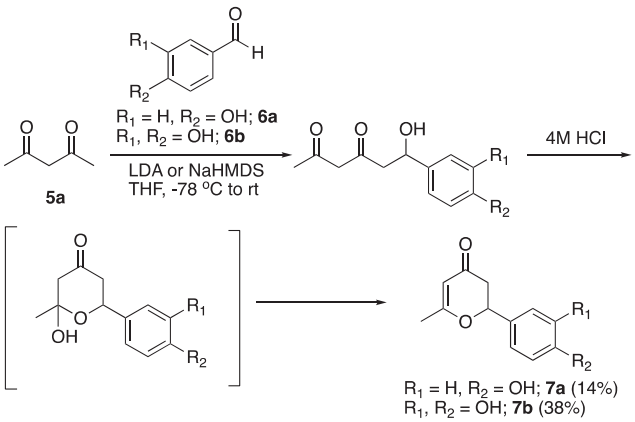

Scheme 1. Preparation of aryl γ-dihydropyrones (**7a-b**).

AY1319 (**2**) the most water soluble C5-curcuminoid from our previous report.[23] The water solubility of 3,4,2′,5′-dicathecol (**9f**) was 2339 μM. In contrast, 3,4,2′,3′-dicathecol (**9e**) showed lowest water solubility. It is noteworthy that the positions of the hydroxy groups on the phenyl rings influenced the water solubility. The ClogP values of the synthesized γ-dihydropyrones (**7a-b, 8a-c, 9a-f**) were similar to those of CUR (**1**), with the exception of monoaryl γ-dihydropyrones **7a** and **7b**. Their tPSA values were also generally "drug like" [26].

Next, the cytotoxicities of the synthesized γ-dihydropyrones (**7a-b, 8a-c, 9a-f**) were ascertained by testing them against highly differentiated rat pheochromocytoma (PC-12) cells in a standard water soluble tetrazolium-8 (WST-8) assay [27]. PC12 cells (1.0×10^4 cells) and each synthesized γ-dihydropyrone (1% solution in DMSO) were co-cultured for 24 h, and then treated with WST-8. We evaluated the eleven synthesized γ-dihydropyrones (**7a-b, 8a-c, 9a-f**) for viability alongside CUR (**1**), which served as the control (CC_{50} = 52 μM). Surprisingly, all γ-dihydropyrones (**7a-b, 8a-c, 9a-f**) were significantly less cytotoxic than either CUR (**1**) or AY1319 (**2**) (Table 1). The cytotoxicity of **9f** against PC-12 cells is shown in Fig. 2A. Diaryl γ-dihydropyrone (**9f**) at a concentration of 20 μM was not apparently cytotoxic against PC-12 cells. In contrast, PC-12 cells have hardly survived at 150 μM of **9f**. Diaryl γ-dihydropyrone (**9f**) exhibited moderate cytotoxicity with an IC_{50} value of 114 μM based on inspection of the sigmoidal curve.

The anti Aβ aggregation activity of CUR (**1**) was investigated using the popular ThT method [28]. Fresh Aβ(1–42) (25 μM) was incubated at 37 °C with ThT and the fluorescence of the mixture measured over time. The fluorescence was found to follow a sigmoidal-like curve, with a point of inflection (Fig. 2B). The initial lag time of about 2 h is thought to correspond to the aggregation of monomeric Aβ(1–42) to oligomer and/

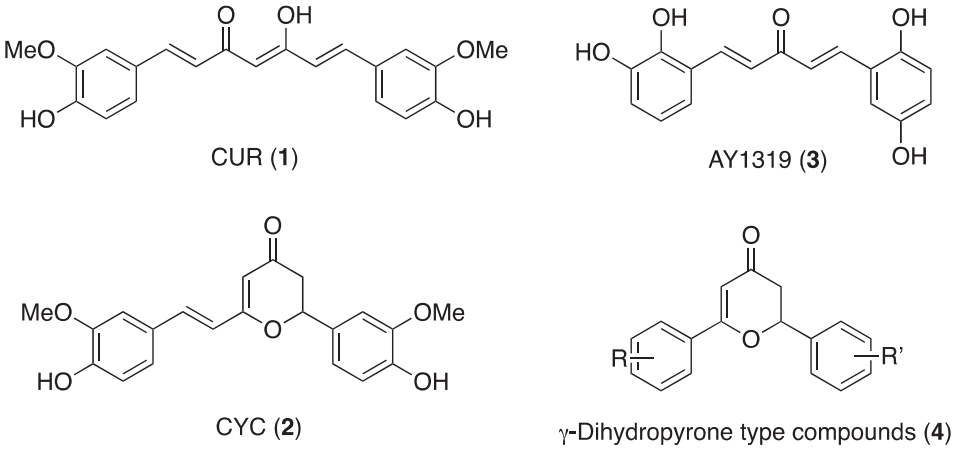

Fig. 1. Chemical structure of three curcuminoids (**1**–**3**) and diaryl γ-dihydropyrones (**4**).

or protofibrils; and the sharp increase in fluorescence at about 6 h to the aggregation of protofibrils to amyloid fibrils. The extent of Aβ(1–42) aggregation after 20 h was defined to be 100% (blue curve; control). Incubation of a mixture of 25 μM monomeric Aβ(1–42) and 10 μM CUR (**1**) at 37 °C resulted in a similar sigmoidal-like curve with a final equilibrium level of ~20% (orange curve). Thus, CUR (**1**) at a concentration of 10 μM was found to inhibit Aβ aggregation (25 μM) at a ratio of 80%, a result similar to that previously reported [21]. In addition, the final equilibrium level at 20 h of the mixture of 25 μM Aβ(1–42) and 1 μM CUR (**1**) showed ~60% (40% inhibition) (gray curve). All the synthesized γ-dihydropyrones (**7a-b, 8a-c, 9a-f**) were individually tested in this assay. 10 μM of the γ-dihydropyrones **7b**, **8b** and **9a-f** bearing a catechol moiety exhibited an aggregation inhibition rate of 50% or more for all derivatives except **9c**. Therefore, the catechol moiety was concluded to play an important role in Aβ aggregation inhibition. In addition, the inhibition rate of diaryl γ-dihydropyrones **9a**, **9e**, and **9f** bearing an *ortho*-hydroxyl group was higher than for CUR (**1**), and reached 100% for diaryl γ-dihydropyrones **9e** and **9f**. It is noteworthy that derivatives incorporating a combination of a hydroxyl group at the ortho position and either 2,3- or 2,5-catechol moieties were also effective.

A similar experiment using 1 μM of selected derivatives was performed. Many showed an inhibition rate of about 40%, similarly to that of CUR (**1**). The inhibition rate associated with diaryl γ-dihydropyrone (**9e**), 100% at 10 μM, decreased significantly to 52% at 1 μM. On the other hand, diaryl γ-dihydropyrone (**9f**) demonstrated an inhibition rate of 100% at 10 μM (yellow curve) and showed a favorable inhibition rate of 76% even at 1 μM (sky blue curve) – exceeding that of both CUR (**1**) and AY1319 (**2**) (Fig. 2B, Table 1). Using the IC_{50} values of CUR (**1**) (4.11 μM) as a control, the IC_{50} values of three selected γ-dihydropyrones (**8c, 9e and 9f**) were ascertained and found to be 3.88, 2.32 and 3.81 μM, respectively. Thus, **8c**, **9e** and **9f** are concluded to be good inhibitors, demonstrating a relatively narrow range of IC_{50}.

These results were obtained using racemic sample of the γ-dihydropyrone derivatives. Optical resolution of racemic diaryl γ-dihydropyrone (**9f**), which had the highest anti Aβ aggregation inhibition activity, was performed using an HPLC equipped with a chiral column. After much experimentation, two clear peaks (Rt = 6.8 min for low polar **9f** and 22.7 min for high polar **9f**) were obtained using a CHIRALCEL AD-H column; the optical rotations of which were −448° and +396°, respectively (Fig. 2C). The separate evaluation of the Aβ aggregation inhibitory of each enantiomer (-)- **9f** and (+)- **9f** was attempted. No significant differences in the rate of aggregation inhibition were observed (64% for 1 μM of low polar (−)- **9f**, 75% for 1 μM of high polar (+)-**9f** and the racemate **9f** (74% for 1 μM). Thus, the relative stereochemistry of (−)- **9f** and (+)- **9f** was concluded not to affect Aβ aggregation inhibition (Fig. 2D).

CUR (**1**) is known to be rapidly hydrolyzed at neutral and alkaline pH, and its bioavailability is too low for it to be a drug candidate. Accordingly, the stability of aqueous solutions of our derivatives was of great interest. To evaluate the aqueous stability of diaryl γ-dihydropyrone (**9f**), a dispersion of it in phosphate buffer (pH 7.5, 500 mM), was shaken at 37 °C for 12 h, desalted, and analyzed by HPLC (Fig. 3). Similar experiments were also performed on CUR (**1**) and AY1319 (**2**), for comparison. HPLC peaks corresponding to CUR (**1**) and AY1319 (**2**) were observed to decrease in intensity, and new peaks (assumed to correspond to decomposition products) were detected after 12 h. On the other hand, diaryl γ-dihydropyrone (**9f**) was stable in this condition shown in Fig. 3.

TEM studies were undertaken, to investigate the morphology of the Aβ aggregation and its inhibition by γ-dihydropyrones. Mature amyloid fibrils with a length of 1 μm or more could be readily discerned (Fig. 4a). A similar morphology was visualized upon treatment of the Aβ fibrils with ThT in a 4:1 ratio (Fig. 4b) the Aβ fibril/ThT complex gave rise to a green signal by fluorescence microscopy. Interestingly, upon incubation of this mixture with diaryl γ-dihydropyrone (**9f**), these fibrils were transformed into small fragments, solutions of which were less fluorescent than those of the fibrils (Fig. 4c, d) presumably due to binding between diaryl γ-dihydropyrone (**9f**) with the protofibrils and/or the amyloid fibrils. Time serial images of TEM of Aβ aggregation were obtained at different time points (0, 2, 4, 8 and 20 h); the images indicated small aggregation at early incubation times, as did the TEM image of Aβ with **9f** (see supporting information Figure S1).

The CD spectra of Aβ with diaryl γ-dihydropyrone (**9f**) suggested it to take the form of a random coil structure, from which inferred that Aβ fibrils are destroyed in the presence of diaryl γ-dihydropyrone (**9f**) (Fig. 4e). The formation of Aβ oligomers was also investigated using dynamic light scattering (DSL). Results from the DSL experiment (Fig. 4f) showed the assembly of the Aβ monomers into structure with a hydrodynamic diameter of 76 nm after 20 h. In contrast, Aβ monomers in the presence of **9f** formed a similar structure with a 0.8 nm hydrodynamic diameter. It is noted that **9f** inhibited the formation of Aβ aggregation to give the oligomers and/or nano-lod like structures.

To better understand the mechanism of Aβ fibril binding, a molecular docking analysis was undertaken. GOLD software (the Cambridge Crystallographic Center) [29] was used to simulate the docking mode of (*R*)- and (*S*)-diaryl γ-dihydropyrones (**9f**) on a 12-fold Aβ(11–42) fibril structure (PDBID:2MXU). Aβ aggregates are composed of hydrophilic and hydrophobic parts, of which the latter forms a pocket-like structure. Previous studies have shown that compounds that bind to and inhibit

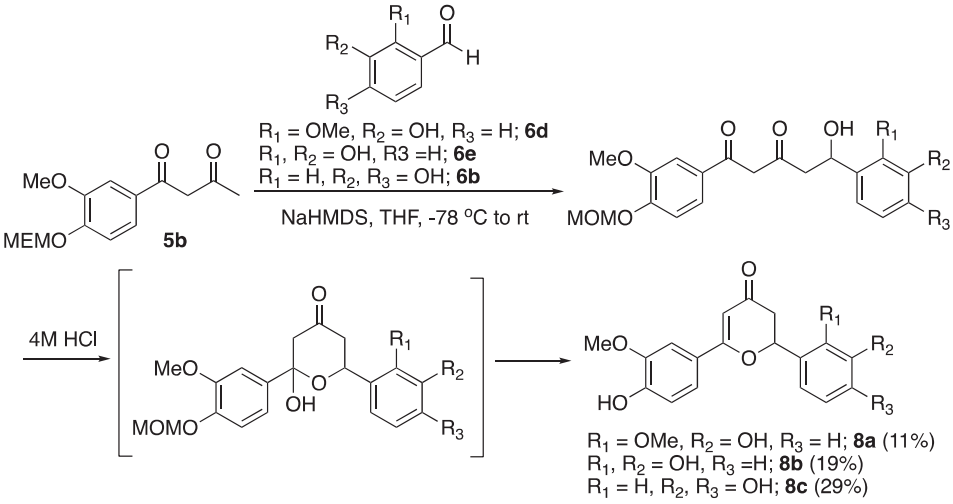

Scheme 2. Preparation of diaryl γ-dihydropyrones (**8a-c**).

aggregation of Aβ aggregates interact with the hydrophilic portion of Aβ. The simulation confirmed that both of (*R*)- and (*S*)-diaryl γ-dihydropyrones (**9f**) interacted with the hydrophilic part of the Aβ aggregate, consistent with the results of previous studies. Residues 16 to 20 of Aβ (Lys-Leu-Val-Phe-Phe) are known to play a critical role in its aggregation, and therefore the extent to which the compounds tested could bind to the sequence correlated with their inhibition of Aβ aggregation (Fig. 5a). (*S*)-Diaryl γ-dihydropyrone **{**(*S*)-**9f}** was found to interact with Val18, Phe19, Phe20, and Glu22; from which it was inferred that it could specifically bind to the Lys-Leu-Val-Phe-Phe sequence, effectively disrupting Aβ aggregation (Fig. 5b). (*R*)-diaryl γ-dihydropyrone **{**(*R*)-**9f}** also interacted with the same core motif (data not shown). Two phenolic rings of enantiomers of **9f** were identified to the comparison of the stable conformers of **9f** by the molecular mechanism experiments.

In summary, a series of diarylpyrone derivatives derived from CYC (**2**) has been designed, synthesized, and evaluation as Aβ aggregation inhibitors. This work resulted in the discovery of AY1511 (**9f**), which incorporates two phenolic rings bearing hydroxy groups at the at 3,4,2′,5′-positions, and exhibits the potent Aβ aggregation inhibitor at a concentration of 1 μM, good water solubility, and good stability. Optimization of the diaryl γ-dihydropyrone framework, and a more detailed structure activity relationship study of diarylpyrone derivatives are underway.

3. Experimental

3.1. General

Reagents were purchased from Nacalai Tesque, Wako Pure Chemical Industries, Ltd., Kanto Chemical Co., Ltd., and Tokyo Chemical Industry Co., Ltd., Aβ (1–42) peptide was purchased from Peptide Research Institute, Ltd. THF was dried and purified by distillation over sodium with benzophenone. CH_2Cl_2 was dried and purified by distillation over CaH_2. Other solvents were used as supplied. Solution phase reactions were monitored by thin layer chromatography (Merck Silica gel 60 F254) on glass plates and visualized with p-anisaldehyde and heating. Column chromatography was performed using spherical, neutral silica gel of diameter 63–210 μm (Kanto chemical co. Inc., Tokyo, Japan). ^1H (500 or 600 MHz) and ^{13}C NMR (125 or 150 MHz) spectra were recorded on either a JNM-ECX500 or JNM-ECX600 (JEOL, Tokyo, Japan). Chemical shifts are reported in ppm relative to tetramethylsilane (0 ppm), chloroform (7.26 ppm: 1H, 77.1 ppm: 13C), methanol (3.31 ppm: 1H, 49.0 ppm: 13C), and dimethyl sulfoxide (2.50 ppm: 1H, 39.6 ppm: 13C). IR spectra were recorded on a FT/IR-460 plus (JASCO, Tokyo, Japan). Mass spectra (ESI-MS) were carried out using the AccuTOF JMS-T100LC (JEOL, Tokyo, Japan). High performance liquid chromatography (HPLC) analyses were carried out using a HITACHI Lachrom ELITE system (Pump: L-2130, UV detector: L-2400), and a Cosmosil 5C18-AR-II column (either 4.6 × 150 mm or 10 × 250 mm for preparative work) (Nacalai Tesque, Kyoto, Japan) eluting with aqueous solutions of MeCN containing 0.1% TFA and detected at OD 256 nm. The chiral column was used a DAICEL CHIRALCEL AD-H (0.46 cmΦ × 25 cm); detection was performed at an OD of 256 nm, and elution was performed with 15% solution of 2-propanol in hexane. Optical rotation measurements were acquired on a JASCO DIP-371. CD spectra were recorded on a J-820 (JASCO, Tokyo, Japan). TEM images were obtained with a JSM7600FA (JEOL, Tokyo, Japan) using ELS-C10 grid (STEM Cu 100 P grid specification grid pitch 100 μm). Electron dying was carried out using 2% tungsten phosphate buffer solution (pH 7.0). Melting points were recorded on an ATM-02 (AS ONE, Tokyo, Japan) and are uncorrected. Fluorescent images by microplate reader were obtained with a Tecan Infinite F200 Pro and measured at an excitation wavelength of 430 nm and fluorescence wavelength of 485 nm (Tecan, Männedorf, Switzerland). For the cytotoxicity evaluation microplate reader, an MTP-310 absorbance microplate reader (CORONA, Hitachi-Naka, Japan) was used to measure the absorbance at wavelengths of 450 nm and 630 nm. Fluorescence measurements were carried out on a FP-8200 (JASCO, Tokyo, Japan). The absorbance was measured by U-3000 or U-1900 (Hitachi, Tokyo, Japan).

3.1.1. 2,3-Dihydro-2-(4-hydroxyphenyl)-6-methyl-4H-pyran-4-one (7a)

A solution of LDA in THF (1.34 mL, 12.5 mmol) was added to a solution of acetylacetone **5a** (511 μL, 5.00 mmol) in THF (15 mL) at −78 °C under a nitrogen atmosphere. After 1 h, the reaction mixture was diluted with 4-hydroxybenzaldehyde **6a** (611 mg, 5.00 mmol) in THF (2 mL) and allowed to slowly warm to room temperature, with stirring.

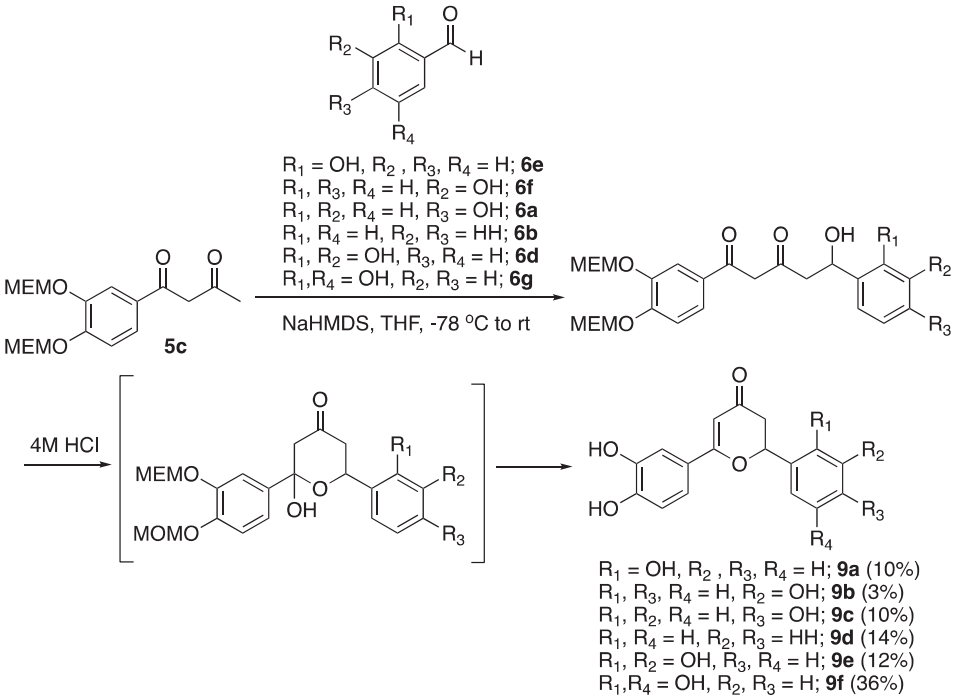

Scheme 3. Preparation of diaryl-γ-dihydropyrones (**9a-f**).

Table 1
The aggregation inhibitory activity, water solubility, ClogP, PSA and cytotoxicity of the synthesized γ-dihydropyrones (**7a-b**, **8a-c**, **9a-f**).

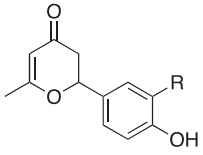

7a: R = H
7b: R = OH

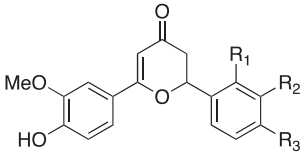

8a: R_1 = H, R_2 = OMe, R_3 = OH
8b: R_1, R_2 = OH, R_3 = H
8c: R_1 = H, R_2, R_3 = OH

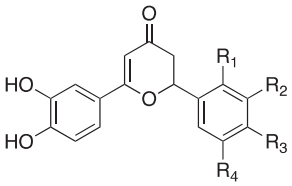

9a: R_1 = OH, R_2, R_3, R_4 = H
9b: R_1, R_3, R_4 = H, R_2 = OH
9c: R_1, R_2, R_4 = H, R_3 = OH
9d: R_1, R_4 = H, R_2, R_3 = OH
9e: R_1, R_2 = OH, R_3, R_4 = H
9f: R_1, R_4 = OH, R_2, R_3 = H

Entry	Compound	Aggr. IN. (%)[b] 10 μM	1 μM	Solubility(μM)[a]	CLogP	PSA	CytotoxicityIC_{50} (μM)
1	CUR (**1**)	80	40	0.19	2.17	96.22	52
2	AY1031	100	62	31	2.03	97.99	–
3	AY1319 (**2**)	100	46	271	2.46	97.99	59
4	**7a**	0	–	2714	0.6	46.53	>150
5	**7b**	57	40	3104	0.21	66.76	>150
6	**8a**	26	–	706	2.03	85.22	103
7	**8b**	84	48	557	1.77	96.22	>150
8	**8c**	72	60	1126	1.77	96.22	>150
9	**9a**	68	41	259	1.89	86.99	149
10	**9b**	62	42	851	1.89	86.99	141
11	**9c**	40	–	621	1.89	86.99	>150
12	**9d**	71	26	668	1.5	107.22	142
13	**9e**	100	52	58	1.5	107.22	129
14	AY1511 (**9f**)	100	76	2339	1.5	107.22	114

[a] Water solubilities were measured by the "shake flash" method [25].
[b] Aggregation inhibition values of Aβ(1–42) after a 20 h incubation at 25 μM were indicated using 1 μM inhibitors and calculated based on the ThT-based fluorescence spectroscopy assay (excitation = 440 nm, emission = 490 nm). Values are mean values from three independent experiments.

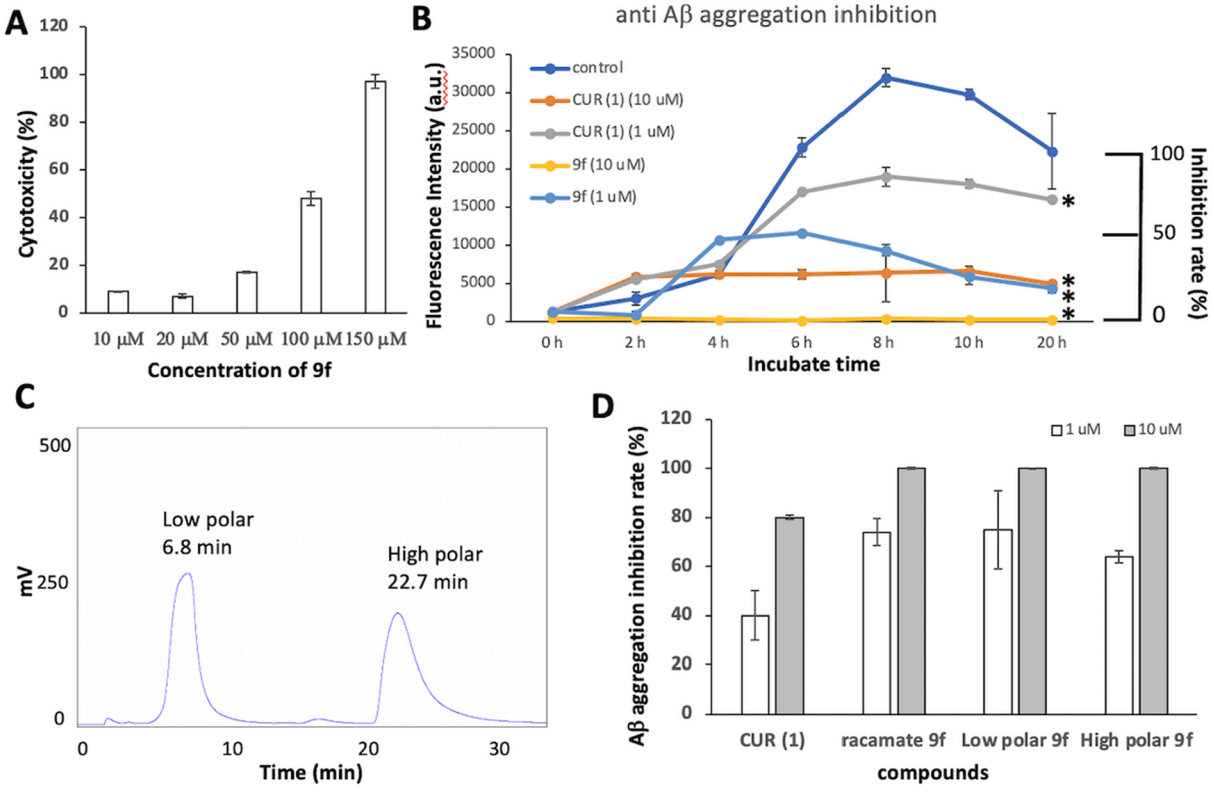

Fig. 2. (A) Cytotoxicity of diaryl γ-dihydropyrone (**9f**) by WST-8 assay. (B) Time course of anti Aβ aggregation inhibition of CUR (**1**) and diaryl γ-dihydropyrone (**9f**). (C) Normal phase HPLC chart of (−)-**9f** for low polar and (+)-**9f** for high polar (CHIRALCEL AD-H 0.46 cm Φ × 25 cm, Flow rate: 1.5 mL/min, hexane/2-propanol = 85:15 isocratic). (D) Aggregation inhibition rate when adding each derivative (both enantiomers of (−)- **9f** and (+)- **9f**, racemate **9f** and CUR (**1**) to Aβ(1–42) (25 μM). Values and error bars correspond to the average and standard deviation of three measurements, *$p < 0.05$ versus control.

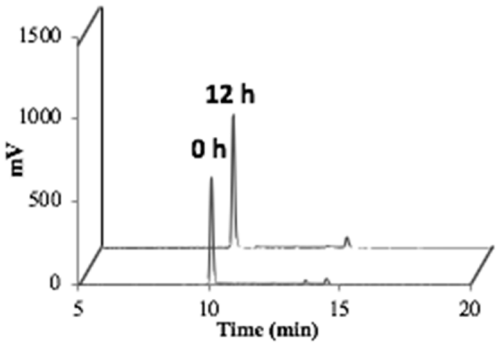

Fig. 3. (A) HPLC chart of diaryl γ-dihydropyrone (**9f**) before (0 h) and after shaking for 12 h (UV: 256 nm, 0.1 mg/mL (MeOH) 20 μL injection to HPLC).

After for 12 h, 4 M HCl (15 mL) was added and the mixture stirred for 15 min. The reaction mixture was added to brine and extracted with AcOEt. The obtained organic layer was washed with brine, dried over $MgSO_4$, and concentrated *in vacuo*. The residue was purified with silica gel column chromatography (97:3 = $CHCl_3$:MeOH) to afford **7a** (144 mg, 706 μmol, 14%) as white powder. mp = 160–161 °C. ^{1}H NMR (600 MHz, MeOH-d_4): δ 1.96 (s, 3H), 2.33 (dd, J = 16.8, 2.4 Hz, 1H), 2.81 (dd, J = 16.8, 14.4 Hz, 1H), 5.32 (s, 1H), 5.33 (dd, J = 14.4, 2.4 Hz, 1H), 6.73 (d, J = 7.8 Hz, 2H), 7.25 (d, J = 7.8 Hz, 2H), 9.56 (brs, 1H). ^{13}C NMR (150 MHz, MeOH-d_4): δ 19.9, 41.3, 81.0, 103.8, 115.0, 115.6, 127.9, 129.0, 132.2, 157.8, 176.6, 191.5. IR (film) ν_{max} cm^{-1}: 3170, 2966, 2881, 2826, 1675, 1599, 1519, 1456, 1399, 1218, 1159, 994, 833, 665, 605. ESIHRMS *m/z*: calcd. for $C_{12}H_{12}O_3Na$ $[M+Na]^+$ 227.0684, found: 227.0681.

3.1.2. 2,3-Dihydro-2-(3,4-dihydroxyphenyl)-6-methyl-4H-pyran-4-one (7b)

A solution of 40% NaHMDS in THF (15.0 mL, 30.0 mmol) was added to a solution of acetylacetone **5a** (511 μL, 5.00 mmol) in THF (10 mL) at −78 °C under a nitrogen atmosphere. After 2 h, the reaction mixture was diluted with 3,4-dihydroxybenzaldehyde **6b** (400 mg, 2.90 mmol) in THF (8 mL) and allowed to slowly warm to room temperature with stirring. After 23 h, 4 M HCl (20 mL) was added and stirred for 20 min. The reaction mixture was added to brine and extracted with AcOEt. The obtained organic layer was washed with brine, dried over $MgSO_4$, and concentrated *in vacuo*. The residue was purified with silica gel column chromatography (1:1 = hexane:AcOEt) to afford **7b** (244 mg, 1.11 mmol, 38%) as white powder. mp = 154–155 °C. ^{1}H NMR (400 MHz, MeOH-d_4): δ 1.96 (s, 3H), 2.33 (dd, J = 16.8, 3.2 Hz, 1H), 2.73 (dd, J = 16.8, 13.6 Hz, 1H), 5.26 (dd, J = 13.6, 3.2 Hz, 1H), 5.30 (s, 1H), 6.67 (dd, J = 8.4, 1.6 Hz, 1H), 6.70 (d, J = 8.4 Hz, 1H), 6.80 (d, J = 1.6 Hz, 1H), 8.97 (s, 1H), 9.03 (s, 1H). ^{13}C NMR (100 MHz, MeOH-d_4): δ 19.9, 41.4, 81.1, 103.8, 113.4, 114.9, 118.0, 129.7, 145.2, 145.7, 176.5, 194.6. IR (film) ν_{max} cm^{-1}:3374, 3112, 2969, 2918, 1714, 1610, 1583, 1439, 1403, 1364, 1289, 1223, 1189, 1168, 1113, 1001, 902, 801, 665. ESIHRMS *m/z*: calcd. for $C_{12}H_{12}O_4Na$ $[M+Na]^+$ 243.0633, found: 243.0648.

3.1.3. 2,3-Dihydro-2,6-[di(3-methoxy-4-hydroxyphenyl)]-4H-pyran-4-one (8a)

40% NaHMDS (1.30 mL, 2.60 mmol) was added to a solution of 1-(3-Methoxy-4-methoxymethylphenyl)-1,3-butanedione **5b** (90 mg, 378 μmol) in THF (2 mL) at −78 °C under a nitrogen atmosphere. After 1 h, the reaction mixture was diluted with a solution of vanillin **6c** (97 mg, 639 μmol) in THF (2 mL) and allowed to slowly warm to room temperature, with stirring. After 13 h, 4 M HCl (4 mL) was added and stirred for 1 h. The reaction mixture was added to brine and extracted with AcOEt. The obtained organic layer was washed with brine, dried over $MgSO_4$, and concentrated *in vacuo*. The residue was purified with silica gel column chromatography (1:1 = hexane:AcOEt) to afford **8a** (14 mg,

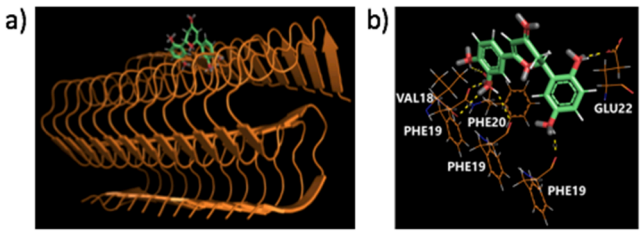

Fig. 5. (a) Binding pose of (*S*)-diaryl γ-dihydropyrone **{**(*S*)-**9f}** in the Aβ fibrils; (b) Detailed view of the docked (*S*)-diaryl γ-dihydropyrone **{**(*S*)-**9f}** structure and the interacting amino acid moieties within the binding site of Aβ fibrils.

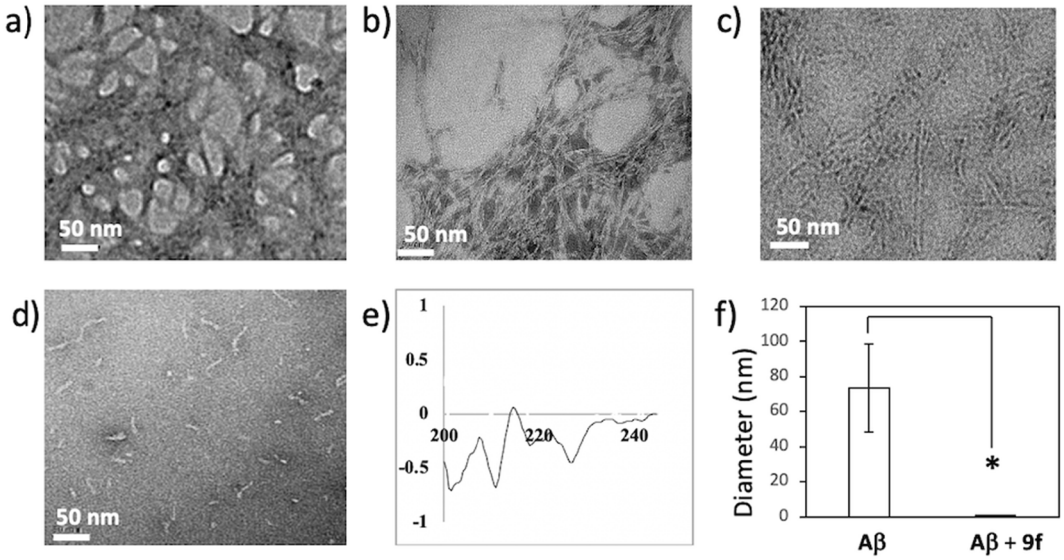

Fig. 4. (a-d) Negative-staining TEM images of Aβ aggregation. (a) Aβ alone after 20 h incubation. (b) Aβ aggregation with ThT after 20 h incubation. (c) Aβ nanorod-like structure with diaryl γ-dihydropyrone (**9f**) after 8 h incubation. (d) Aβ nanorod-like structure with diaryl γ-dihydropyrone (**9f**) after 20 h incubation. Scale bars = 50 nm. (e) CD spectrum of Aβ nanorod-like structure with diaryl γ-dihydropyrone (**9f**). (f) Determination of the size of Aβ oligomers after 20 h incubation using DSL. Values and error bars correspond to the average and standard deviation of three measurements, *$p < 0.05$.

41.8 μmol, 11%) as yellow oil. ^{1}H NMR (500 MHz, MeOH-d_4): δ 2.60 (dd, J = 17.5, 3.5 Hz, 1H), 3.02 (dd, J = 17.0, 13.5 Hz, 1H), 3.84 (s, 3H), 3.86 (s, 3H), 5.51 (dd, J = 13.5, 3.5 Hz, 1H), 6.04 (s, 1H), 6.83 (d, J = 8.5 Hz, 1H), 6.84 (d, J = 8.5 Hz, 1H), 6.97 (dd, J = 8.5, 1.5 Hz, 1H), 7.11 (d, J = 1.5 Hz, 1H), 7.31 (d, J = 2.5 Hz, 1H), 7.35 (dd, J = 8.5, 2.5 Hz, 1H). ^{13}C NMR (125 MHz, MeOH-d_4): δ 41.9, 55.1 (*C*2), 81.2, 99.4, 109.7, 110.1, 114.9, 115.1, 119.4, 121.0, 123.7, 129.8, 147.0, 147.8, 147.9, 150.8, 172.2, 194.9. IR (film) ν_{max} cm^{-1}:3392, 3006, 2963, 2932, 1713, 1652, 1576, 1430, 1363, 1282, 1222, 1125, 1031, 902, 819, 665. ESIHRMS *m/z*: calcd. for $C_{19}H_{17}O_6$ $[M+H]^+$ 343.1182, found: 343.1165.

3.1.4. 2,3-Dihydro-2-(2,3-dihydroxyphenyl)-6-(3-methoxy-4-hydroxyphenyl)-4H-pyran-4-one (8b)

40% NaHMDS (3.80 mL, 7.60 mmol) was added to a solution of 1-(3-Methoxy-4-methoxymethylphenyl)-1,3-butanedione **5b** (300 mg, 1.26 mmol) in THF (5 mL) at −78 °C under a nitrogen atmosphere. After 1 h, the reaction mixture was diluted with 2,3-dihydroxybenzaldehyde **6c** (294 mg, 2.13 mmol) in THF (5 mL) and allowed to slowly warm to room temperature, with stirring. After 18 h, 4 M HCl (13 mL) was added and stirred for 1 h. The reaction mixture was added to brine and extracted with AcOEt. The obtained organic layer was washed with brine, dried over $MgSO_4$, and concentrated *in vacuo*. The residue was purified with silica gel column chromatography (1:1 = hexane:AcOEt) to afford **8b** (79 mg, 240 μmol, 19%) as yellow oil. ^{1}H NMR (600 MHz, MeOH-d_4): δ 2.68 (dd, J = 17.4, 3.6 Hz, 1H), 2.89 (dd, J = 17.4, 14.4 Hz, 1H), 3.85 (s, 3H), 5.88 (dd, J = 14.4, 3.6 Hz, 1H), 6.03 (s, 1H), 6.73 (t, J = 7.8 Hz, 1H), 6.79 (dd, J = 7.8, 1.2 Hz, 1H), 6.83 (d, J = 8.4 Hz, 1H), 6.96 (dd, J = 8.4, 1.2 Hz, 1H), 7.35 (d, J = 1.2 Hz, 1H), 7.36 (dd, J = 7.8, 1.2 Hz, 1H). ^{13}C NMR (150 MHz, MeOH-d_4): δ 40.8, 55.1, 76.6, 99.3, 109.7, 114.8, 115.1, 116.9, 119.3, 121.0, 125.1, 133.8, 142.8, 145.0, 147.8, 150.8, 172.7, 195.2. IR (film) ν_{max} cm^{-1}:3366, 2964, 2932, 2849, 1705, 1634, 1572, 1509, 1430, 1365, 1285, 1205, 1127, 1030, 948, 905, 782, 736, 647, 517. ESIHRMS *m/z*: calcd. for $C_{18}H_{17}O_6$ $[M+H]^+$ 329.1025, found: 329.1021.

3.1.5. 2,3-Dihydro-2-(3,4-dihydroxyphenyl)-6-(3-methoxy-4-hydroxyphenyl)-4H-pyran-4-one (8c)

40% NaHMDS (3.78 mL, 7.56 mmol) was added to a solution of 1-(3-Methoxy-4-methoxymethylphenyl)-1,3-butanedione **5b** (300 mg, 1.26 mmol) in THF (5 mL) at −78 °C under nitrogen atmosphere. After 1 h, the reaction mixture was diluted with a solution of 3,4-dihydroxybenzaldehyde **6b** (294 mg, 2.13 mmol) in THF (5 mL) and allowed to slowly warm to eoom temperature, with stirring. After 17 h, 4 M HCl (10 mL) was added and stirred for 1 h. The reaction mixture was added to brine and extracted with AcOEt. The obtained organic layer was washed with brine, dried over $MgSO_4$, and concentrated *in vacuo*. The residue was purified with silica gel column chromatography (1:2 = hexane:AcOEt) to afford **8c** (119 mg, 363 μmol, 29%) as yellow oil. ^{1}H NMR (600 MHz, MeOH-d_4): δ 2.56 (dd, J = 16.2, 3.6 Hz, 1H), 2.91 (dd, J = 16.2, 13.8 Hz, 1H), 3.81 (s, 3H), 5.40 (dd, J = 13.8, 3.6 Hz, 1H), 6.00 (s, 1H), 6.78 (d, J = 8.4 Hz, 1H), 6.80 (dd, J = 8.4, 2.4 Hz, 1H), 6.80 (d, J = 7.8 Hz, 1H), 6.94 (d, J = 1.8 Hz, 1H), 7.27 (d, J = 1.8 Hz, 1H), 7.31 (dd, J = 7.8, 1.8 Hz, 1H). ^{13}C NMR (150 MHz, MeOH-d_4): δ 41.9, 55.1, 81.0, 99.3, 109.6, 113.5, 115.0, 115.1, 118.1, 121.0, 123.7, 129.9, 145.3, 145.8, 147.7, 150.8, 172.2, 194.9. IR (film) ν_{max} cm^{-1}:3336, 2964, 2925, 2854, 1705, 1635, 1575, 1509, 1457, 1431, 1372, 1287, 1204, 1125, 1030, 905, 815. ESIHRMS *m/z*: calcd. for $C_{18}H_{16}O_6Na$ $[M+Na]^+$ 351.0845, found: 351.0873.

3.1.6. 2,3-Dihydro-2-(2-hydroxyphenyl)-6-(3,4-dihydroxyphenyl)-4H-pyran-4-one (9a)

40% NaHMDS (4.47 mL, 8.94 mmol) was added to a solution of 1-(3,4-dimethoxyethylmethylphenyl)-1,3-butanedione **5c** (300 mg, 1.06 mmol) in THF (5 mL) at −78 °C under a nitrogen atmosphere. After 2 h, the reaction mixture was diluted with a solution of salicylaldehyde **6e** (88 μL, 826 μmol) in THF (2 mL) and allowed to slowly warm to room temperature. After 19 h, 4 M HCl (30 mL) was added and stirred for 1 h. The reaction mixture was added to brine and extracted with AcOEt. The obtained organic layer was washed with brine, dried over $MgSO_4$, and concentrated *in vacuo*. The residue was purified with silica gel column chromatography (1:2 = hexane:AcOEt) to afford **9a** (23 mg, 78.4 μmol, 10%) as yellow oil. ^{1}H NMR (600 MHz, MeOH-d_4): δ 2.70 (dd, J = 16.8, 3.6 Hz, 1H), 2.83 (dd, J = 16.2, 14.4 Hz, 1H), 5.84 (dd, J = 14.4, 3.0 Hz, 1H), 5.98 (s, 1H), 6.80 (d, J = 7.8 Hz, 1H), 6.83 (d, J = 7.8 Hz, 1H), 6.89 (t, J = 7.8 Hz, 1H), 7.18 (t, J = 7.8 Hz, 1H), 7.25 (dd, J = 7.8, 1.8 Hz, 1H), 7.26 (d, J = 1.8 Hz, 1H), 7.48 (d, J = 7.8 Hz, 1H). ^{13}C NMR (150 MHz, MeOH-d_4): δ 40.8, 76.5, 99.0, 113.4, 114.9, 115.1, 119.4, 119.6, 123.8, 125.0, 126.3, 129.2, 145.3, 149.7, 154.2, 172.9, 195.2. IR (film) ν_{max} cm^{-1}: 3252, 2964, 2923, 1599, 1570, 1521, 1457, 1396, 1294, 1198, 1119, 992, 810, 757, 665. ESIHRMS *m/z*: calcd. for $C_{17}H_{15}O_5$ $[M+H]^+$ 299.0919, found: 299.0889.

3.1.7. 2,3-Dihydro-2-(3-hydroxyphenyl)-6-(3,4-dihydroxyphenyl)-4H-pyran-4-one (9b)

40% NaHMDS (2.13 mL, 4.25 mmol) was added to a solution of 1-(3,4-Dimethoxymethylphenyl)-1,3-butanedione **5c** (200 mg, 708 μmol) in THF (5 mL) at −78 °C under a nitrogen atmosphere. After 1 h, the reaction mixture was diluted with a solution of 3-hydroxybenzaldehyde **6f** (87 mg, 708 μmol) in THF (4 mL) and allowed to slowly warm to room temperature, with stirring. After 11 h, 4 M HCl (10 mL) was added and stirred for 1 h. The reaction mixture was added to brine and extracted with AcOEt. The obtained organic layer was washed with brine, dried over $MgSO_4$, and concentrated *in vacuo*. The residue was purified with silica gel column chromatography (1:1 = hexane:AcOEt) to afford **9b** (6 mg, 18.4 μmol, 2.6%) as yellow oil. ^{1}H NMR (600 MHz, MeOH-d_4): δ 2.64 (dd, J = 16.8, 3.0 Hz, 1H), 2.89 (dd, J = 16.2, 13.8 Hz, 1H), 5.52 (dd, J = 13.8, 3.6 Hz, 1H), 5.98 (s, 1H), 6.77 (t, J = 7.8 Hz, 1H), 6.80 (d, J = 9.0 Hz, 1H), 6.95 (s, 1H), 6.96 (d, J = 7.8 Hz, 1H), 7.22 (d, J = 7.8 Hz, 1H), 7.23 (d, J = 7.2 Hz, 1H), 7.25 (s, 1H). ^{13}C NMR (150 MHz, MeOH-d_4): δ 41.8, 80.9, 99.0, 113.4, 113.5, 115.0, 115.1, 118.0, 119.6, 123.7, 128.3, 129.9, 145.3, 145.7, 149.7, 172.4, 194.9. IR (film) ν_{max} cm^{-1}: 3246, 3005, 2959, 2923, 1714, 1601, 1570, 1520, 1444, 1363, 1223, 1117, 911, 812, 665. ESIHRMS *m/z*: calcd. for $C_{17}H_{15}O_5$ $[M+H]^+$ 299.0919.

3.1.8. 2,3-Dihydro-2-(4-hydroxyphenyl)-6-(3,4-dihydroxyphenyl)-4H-pyran-4-one (9c)

40% NaHMDS (2.13 mL, 4.25 mmol) was added to a solution of 1-(3,4-Dimethoxymethylphenyl)-1,3-butanedione **5c** (200 mg, 708 μmol) in THF (5 mL) at −78 °C under a nitrogen atmosphere. After 2 h, the reaction mixture was diluted with 4-hydroxybenzaldehyde **6a** (87 mg, 708 μmol) in THF (4 mL) and allowed to slowly warm to room temperature, with stirring. After 12 h, 4 M HCl (10 mL) was added and stirred for 1 h. The reaction mixture was added to brine and extracted with AcOEt. The obtained organic layer was washed with brine, dried over $MgSO_4$, and concentrated *in vacuo*. The residue was purified with silica gel column chromatography (1:1 = hexane:AcOEt) to afford **9c** (20 mg, 68.4 μmol, 10%) as yellow oil. ^{1}H NMR (600 MHz, MeOH-d_4): δ 2.58 (dd, J = 16.2, 2.4 Hz, 1H), 2.98 (dd, J = 16.2, 13.8 Hz, 1H), 5.50 (dd, J = 13.8, 2.4 Hz, 1H), 6.03 (s, 1H), 6.84 (d, J = 9.0 Hz, 1H), 6.87 (d, J = 9.0 Hz, 2H), 7.26 (d, J = 1.8 Hz, 1H), 7.25 (dd, J = 9.0, 1.8 Hz, 1H), 7.39 (d, J = 9.0 Hz, 2H). ^{13}C NMR (150 MHz, MeOH-d_4): δ 41.7, 80.8, 99.0, 113.4, 115.1 (*C*2), 119.6, 123.6, 127.9 (*C*2), 129.2, 145.2, 149.7, 157.9, 171.7, 172.5, 195.0. IR (film) ν_{max} cm^{-1}:3333, 2964, 2927, 1710, 1598, 1517, 1444, 1364, 1292, 1223, 1172, 1119, 989, 835, 665. ESIHRMS *m/z*: calcd. for $C_{17}H_{15}O_5$ $[M+H]^+$ 299.0919, found: 299.0931.

3.1.9. 2,3-Dihydro-2,6-[di(3,4-dihydroxyphenyl)]-4H-pyran-4-one (9d)

40% NaHMDS (4.47 mL, 8.94 mmol) was added to a solution of 1-(3,4-dimethoxyethoxymethylphenyl)-1,3-butanedione **5c** (200 mg, 708

μmol) in THF (5 mL) at −78 °C under a nitrogen atmosphere. After 1 h, the reaction mixture was diluted with 3,4-dihydroxybenzaldehyde **6b** (112 mg, 810 μmol) in THF (2 mL) and allowed to warm to room temperature. After 12 h, 4 M HCl (23 mL) was added and stirred for 20 min. The reaction mixture was added to brine and extracted with AcOEt. The obtained organic layer was washed with brine, dried over $MgSO_4$, and concentrated *in vacuo*. The residue was purified with silica gel column chromatography (1:1 = hexane:AcOEt) to afford **9d** (35 mg, 112 μmol, 14%) as yellow oil. ^{1}H NMR (600 MHz, MeOH-d_4): δ 2.57 (dd, J = 16.8, 3.6 Hz, 1H), 2.92 (dd, J = 16.8, 13.8 Hz, 1H), 5.42 (dd, J = 13.8, 3.6 Hz, 1H), 5.95 (s, 1H), 6.79 (d, J = 8.4 Hz, 2H), 6.83 (dd, J = 7.8, 2.4 Hz, 1H), 6.95 (d, J = 1.8 Hz, 1H), 7.22 (dd, J = 7.8, 1.8 Hz, 1H), 7.23 (d, J = 2.4 Hz, 1H). ^{13}C NMR (150 MHz, MeOH-d_4): δ 41.8, 80.9, 99.0, 113.4, 113.5, 115.0, 115.1, 118.1 (*C*2), 119.6, 123.7, 129.9, 145.2, 145.7, 149.7, 172.5, 195.0. IR (film) ν_{max} cm^{-1}:3275, 3001, 2964, 2918, 1714, 1601, 1570, 1520, 1447, 1363, 1292, 1119, 993, 912, 814, 665. ESIHRMS *m/z*: calcd. for $C_{17}H_{15}O_6$ $[M+H]^+$ 315.0869, found: 315.0870.

3.1.10. 2,3-Dihydro-2-(2,3-dihydroxyphenyl)-6-(3,4-dihydroxyphenyl)-4H-pyran-4-one (9e)

40% NaHMDS (4.47 mL, 8.94 mmol) was added to a solution of 1-(3,4-dimethoxyethylmethylphenyl)-1,3-butanedione **5c** (300 mg, 1.06 mmol) in THF (5 mL) at −78 °C under a nitrogen atmosphere. After 1 h, the reaction mixture was diluted with 2,3-dihydroxybenzaldehyde **6d** (112 mg, 810 μmol) in THF (2 mL) and allowed to slowly warm to room temperature. After 13 h, 4 M HCl (20 mL) was added and stirred for 30 min. The reaction mixture was added to brine and extracted with AcOEt. The obtained organic layer was washed with brine, dried over $MgSO_4$, and concentrated *in vacuo*. The residue was purified with silica gel column chromatography (1:2 = hexane:AcOEt) to afford **9e** (31 mg, 98.0 μmol, 12%) as yellow powder. mp 158–159 °C. ^{1}H NMR (600 MHz, MeOH-d_4): δ 2.68 (dd, J = 17.4, 3.6 Hz, 1H), 2.86 (dd, J = 16.8, 13.8 Hz, 1H), 5.85 (dd, J = 13.8, 3.6 Hz, 1H), 5.97 (s, 1H), 6.73 (t, J = 7.8 Hz, 1H), 6.78 (d, J = 7.8 Hz, 1H), 6.80 (d, J = 8.4 Hz, 1H), 6.97 (d, J = 7.8 Hz, 1H), 7.24 (dd, J = 8.4, 1.2 Hz, 1H), 7.25 (d, J = 1.2 Hz, 1H). ^{13}C NMR (150 MHz, MeOH-d_4): δ 40.8, 76.5, 99.0, 113.4, 114.7, 115.1, 116.9, 119.3, 119.6, 123.8, 125.2, 142.7, 144.9, 145.3, 149.7, 172.9, 195.3. IR (film) ν_{max} cm^{-1}:3177, 3006, 2964, 2927, 1714, 1567, 1520, 1362, 1289, 1221, 1121, 1027, 963, 914, 665. ESIHRMS *m/z*: calcd. for $C_{17}H_{15}O_6$ $[M+H]^+$ 315.0869, found: 315.0871.

3.1.11. 2,3-Dihydro-2-(2,5-dihydroxyphenyl)-6-(3,4-dihydroxyphenyl)-4H-pyran-4-one (9f)

40% NaHMDS (4.47 mL, 8.94 mmol) was added to a solution of 1-(3,4-dimethoxymethylphenyl)-1,3-butanedione **5c** (300 mg, 1.06 mmol) in THF (5 mL) at −78 °C under a nitrogen atmosphere. After 2 h, the reaction mixture was diluted with 2,5-dihydroxybenzaldehyde **6 g** (146 mg, 1.06 mmol) in THF (2 mL) and allowed to slowly warm to room temperature. After 16 h, 4 M HCl (20 mL) was added and stirred for 3 h. The reaction mixture was added to brine and extracted with AcOEt. The obtained organic layer was washed with brine, dried over $MgSO_4$, and concentrated *in vacuo*. The residue was purified with silica gel column chromatography (1:2 = hexane:AcOEt) to afford **9f** (121 mg, 384 μmol, 36%) as yellow oil. ^{1}H NMR (600 MHz, MeOH-d_4): δ 2.70 (dd, J = 16.2, 3.0 Hz, 1H), 2.76 (dd, J = 16.2, 13.8 Hz, 1H), 5.78 (dd, J = 13.8, 3.0 Hz, 1H), 5.97 (s, 1H), 6.62 (dd, J = 9.0, 3.0 Hz, 1H), 6.67 (d, J = 8.4 Hz, 1H), 6.81 (d, J = 9.0 Hz, 1H), 6.96 (d, J = 3.0 Hz, 1H), 7.26 (dd, J = 8.4, 3.0 Hz, 1H), 7.27 (d, J = 3.0 Hz, 1H). ^{13}C NMR (150 MHz, MeOH-d_4): δ 40.9, 76.4, 99.0, 112.6, 113.4, 115.1, 115.5, 115.8, 119.6, 123.8, 125.8, 145.3, 146.8, 149.7, 150.1, 172.8, 195.1. IR (film) ν_{max} cm^{-1}:3278, 2975, 1702, 1599, 1571, 1509, 1450, 1366, 1297, 1268, 1201, 1121, 1002, 911, 811, 665. ESIHRMS *m/z*: calcd. for $C_{17}H_{15}O_6$ $[M+H]^+$ 315.0869, found: 315.0856.

3.2. Aqueous solubility test

The aqueous solubility of the compounds was ascertained using the shake flask method. Briefly, about 1 mg of each compound was dispersed in 1.0 mL of water. The suspension was shaken for 12 h at 37 °C. An aliquot was filtered through a Millipore Cosmo Spin Filter H (0.45 μm). The filtrate was diluted in MeOH and injected into an HPLC with UV detection; peak heights were recorded at 400 nm or 256 nm. The concentration of the sample solution was calculated using a previously determined calibration curve, corrected for the dilution factor of the sample.

3.3. Assay of Aβ aggregation inhibitory activity

The extent to which the synthesized compounds could inhibit Aβ aggregation was assessed with the ThT method. Briefly, 25 μM Aβ(1–42) (Peptide Institute, Inc.; Ibaraki, Japan) was combined with 0 μM (control) or 10 or 1 μM curcumin analog in the presence of 50 mM sodium phosphate buffer, pH 7.5, 100 mM NaCl, 1% (v/v) DMSO. The total fluid volume was 25 μL. Reactions were incubated at 37 °C. To monitor amount of Aβ aggregate, aliquots were diluted fourfold into 5 μM ThT and immediately evaluated for fluorescence (excitation = 445 nm, emission = 490 nm).

3.4. Aβ aggregation dissociation evaluation

A 25 μM solution of Aβ (1–42) in H_2O was mixed with 50 μM phosphate buffer (pH 7.5) and 100 μM NaCl. The reaction solution was incubated at 37 °C for 20 h, 10 μM derivative and 5 μM ThT solution were added, and the fluorescence intensity was measured and evaluated using a fluorescent plate reader (Ex: 430 nm, Em: 485 nm).

3.5. CD spectra

The Aβ aggregation inhibitory activity evaluation solution (100 μL) was diluted with pure water (200 μL), and the CD spectrum was measured at a wavelength of 250–200 nm (cell response 2 *sec*, scanning speed 50 nm/min, data acquisition interval 0.5 nm, integration frequency 1, bandwidth 10 nm).

3.6. Transmission electron microscopy (TEM) experiments

A carbon-coated copper grid was overlaid with a suspension of Aβ fibrils and then blotted dry with a filter paper. The grids were washed, negatively stained with 1% phosphotungstate acid and dried in air before being examined in a JEM-2100 transmission electron microscope at an accelerating voltage of 200 kV.

3.7. Evaluation of the cytotoxicity by MTT assay

PC12 cells were maintained in a suspension culture of DMEM supplemented with 5% FBS (Fetal Bovine Serum) containing 1% of a penicillin-streptomycin (1:1) mixture. A 100 μL aliquot of PC12 cells (10000 cells/ml) was added to a 96 well plate and incubated for 24 h at 37 °C in a humidified incubator containing 5% CO_2 in air. After 24 h, a 10 μL aliquot of compound CUR analogues (concentrations varying in the range of 1.0–150 μM) was added to each of the 96 wells and incubated for 24 h. A 10 μL WST-8 solution (mixture of WST-8 and 1-Methoxy PMS) was added to each well and the incubation continued for 2 h. The visible absorbance at 450 nm and 630 nm as the reference wavelength of each well was quantified using a microplate reader.

3.8. Underwater stability evaluation

The derivative (1 mg) was dispersed in 50 mM phosphate buffer (pH 7.5) (1 mL) and shaken at 37 °C for 12 h. After desalting with a Seppak,

the mixture was concentrated by centrifugation. It was dissolved in MeOH to adjust to 0.1 mg/ml and subjected to HPLC analysis (flow rate 1 mL/min, 0–30 min, 10–90% CH_3CN/H_2O). The evaluation was performed by comparing with the HPLC peak of a 0.1 mg/ml MeOH solution prepared in advance and analyzing the appearance of a new peak and the difference in the peak area ratio.

3.9. Docking experiment

The 3D coordinates of Aβ fibrils were cited from the Protein data bank (PDB ID: 2MXU). The ligand was docked into the binding sites of Aβ fibrils as assigned to CA Phe-20 (20 Å) by GOLD software and visualized by PyMOL software.

3.10. DLs

A 1 mL solution of Aβ solution (25 μM Aβ, 5 mM sodium phosphate buffer, pH 7.5, 10 mM NaCl, 0.1% (v/v) DMSO) was prepared as previously described and extruded through a polycarbonate membrane with a pore size of 200 nm (Sartorius, Germany) using a Minisart syringe filter (Sartorius). Dynamic light scattering measurements were performed immediately after preparation and after 20 h to track to oligomer size over time. DSL measurements were performed using a Malvern Zetasizer with a glass cuvette.

Author contributions

The manuscript was written through contributions of all authors. All authors have given approval to the final version of the manuscript.

Declaration of Competing Interest

The authors declare that they have no known competing financial interests or personal relationships that could have appeared to influence the work reported in this paper.

Acknowledgements

This work was supported in part by YU-COE (C) program of Yamagata University.

Appendix A. Supplementary data

Supplementary data to this article can be found online at https://doi.org/10.1016/j.bioorg.2020.104302.

References

[1] G.F. Genvais, D. Xu, S.G. Robertson, P.J. Vaillancourt, Y. Zhu, J. Huang, A. LeBlanc, D. Smith, M. Riqby, M.S. Sheaman, E.E. Clarke, H. Zheng, L.H. Van Der Ploeq, S.C. Ruffolo, N.A. Thormberry, S. Xanthoudakis, R.J. Zambori, S. Roy, D. W. Nicholson, Involvement of caspases in proteolytic cleavage of Alzheimer's amyloid-beta precursor protein and amyloidogenic a beta peptide formation, Cell 57 (1999) 395–406.
[2] J. Milobedzka, T.S. Kostanecki, V. Lampe, Zur Kenntnis des Curcumins, Ber. Dtsch. Chem. Ges. 43 (2) (1910) 2163–2170.
[3] S.D. Fabricant, R.N. Farnsowrth, The value of plants used in traditional medicine for drug discovery, Health Perspec. 109 (2001) 69–75.
[4] H. Ammon, M. Wahl, Pharmacology of Curcuma longa, Planta Med 57 (01) (1991) 1–7.
[5] T. Masuda, K. Hidaka, A. Shinohara, H. Yamaguchi, Chemical studies on antioxidant mechanism of curcuminoid: analysis of radical reaction products from curcumin, J. Agric. Food Chem. 47 (1999) 71–77.
[6] S. Shishodia, G. Sethi, B.B. Aggarwal, Curcumin: getting back to the roots, Ann. N. Y. Acad. Sci. 1056 (2005) 206–217.
[7] D.R. Siwak, S. Shishodia, B.B. Aggarwal, R. Kurzrock, Curcumin-induced antiproliferative and proapoptotic effects in melanoma cells are associated with suppression of iκB kinase and nuclear factor κB activity and are independent of the B-raf/mitogen-activated/extracellular signal-regulated protein kinase pathway and the ark pathway, Cancer 104 (2005) 879–890.
[8] B.B. Aggarwal, S. Shishodia, Y. Takada, S. Banerjee, R.A. Newman, C.E. Bueso-Ramos, J.E. Price, Curcumin suppresses the paclitaxel-induced nuclear factor-κB Pathway in breast cancer cells and inhibits lung metastasis of human breast cancer in nude mice, Clin. Cancer Res. 11 (2005) 7490–7498.
[9] S. Aggarwal, H. Ichikawa, Y. Takada, S.K. Sandur, S. Shishodia, B.B. Aggarwal, Curcumin (diferuloylmethane) down-regulates expression of cell proliferation and antiapoptotic and metastatic gene products through suppression of ikappabalpha kinase and akt activation, Mol Pharmacol. 69 (2006) 195–206.
[10] J. Bisson, J.B. McAlpine, J.B. Friesen, S.-N. Chen, J. Graham, G.F.J. Pauli, Can invalid bioactives undermine natural product-based drug discovery? J. Med. Chem. 59 (2016) 1671–1690.
[11] (a) M.K. Nelson, L.J. Dahlin, J. Bisson, J. Graham, F.G. Pauli, A M. Walter, The essential medicinal chemistry of curcumin, J. Med. Chem. 60 (2007) 1620-1637. (b) J. Sun, T. Murata, H. Shigemori, Inhibitory activities of phenylpropanoids from Lycopus lucidus on amyloid aggregation related to Alzheimer's disease and type 2 diabetes, J. Nat. Med. 74 (2019) 579-583. (c) T. Hase, S. Shishido, S. Yamamoto, R. Yamashita, H. Nukima, S. Taira, T. Toyoda, K. Abe, T. Hamaguchi, K. Ono, M. Noguchi-Shinohara, M. Yamada, S. Kobayashi, Rosmarinic acid suppresses Alzheimer's disease development by reducing amyloid β aggregation by increasing monoamine secretion. Sci. Rep. 9 (2019) 8711.
[12] A. Mukhopadhyay, N. Basu, N. Ghatak, K.P. Gujral, Anti-inflammatory and irritant activities of curcumin analogues in rats, Agents and Actions 12 (1982) 508–515.
[13] F. Payton-Stewart, P. Sandusky, W.L. Alworth, NMR study of the solution structure of curcumin, J. Nat. Prod. 70 (2007) 143–146.
[14] P. Anand, A.B. Kunnumakkara, R.A. Newman, B.B. Aggarwal, Bioavailability of curcumin: problems and promises, Mol Pharm. 4 (2007) 807–818.
[15] A. Hassaninasab, Y. Hashimoto, K.T. Yokotani, M. Kobayashi, Discovery of the curcumin metabolic pathway involving a unique enzyme in an intestinal microorganism, Proc. Natl. Acad. Sci. 108 (2011) 6615–6620.
[16] (a) M.D. Cas, R. Ghidoni, Dietary curcumin: correlation between bioavailability and health potential, Nutrients 11 (2019) 2147. (b) S.-S. Xie, J. Liu, C. Tang, C. Pang, Q. Li, Y. Qin, X. Nong, Z. Zhang, J. Guo, M. Cheng, W. Tang, N. Liang, N. Jiang, Design, synthesis and biological evaluation of rasagiline-clorgyline hybrids as novel dual inhibitors of monoamine oxidase-B and amyloid-b aggregation against Alzheimer's disease. 202 (2020) 112475.
[17] H. Konno, H. Endo, S. Ise, K. Miyazaki, H. Aoki, A. Sanjoh, K. Kobayashi, Y. Hattori, K. Akaji, Synthesis and evaluation of curcumin derivatives toward an inhibitor of beta-site amyloid precursor protein cleaving enzyme 1, Biooorg. Med. Chem. Lett. 24 (2014) 685–690.
[18] H. Endo, Y. Nikaido, M. Nakadate, S. Ise, H. Konno, Structure activity relationship study of curcumin analogues toward the amyloid-beta aggregation inhibitor, Bioorg. Med. Chem. Lett. 24 (2014) 5621–5626.
[19] (a) M. Hotsumi, M. Tajiri, Y. Nikaido, T. Sato, K. Makabe, H. Konno, Design, synthesis, and evaluation of a water soluble C5-monoketone type curcumin analogue as a potent amyloid β aggregation inhibitor, Bioorg. Med. Chem. Lett. 29 (2019) 2157-2161. (b) M.E. Abouelea, M.A.A. Orabi, R.A. Abdelhamid, M.S.A. Abdelkader, F.M.M. Darwish, M. Hotsumi, H. Konno, Anti-Alzheimer's flavanolignans from Ceiba pentandra aerial parts. Fitoterapia 143 (2020) 104541.
[20] T. Sato, M. Hotsumi, K. Makabe, H. Konno, Design, synthesis and evaluation of curcumin-based fluorescent probes to detect Aβ fibrils, Bioorg. Med. Chem. Lett. 28 (2018) 3520–3525.
[21] F. Kiuchi, Y. Goto, N. Sugimoto, N. Akao, K. Kondo, Y. Tsuda, Nematocidal activity of turmeric: synergistic action of curcuminoids, Chem. Pharm. Bull. 41 (1993) 1640–1643.
[22] A. Simon, D.P. Allais, J.L. Duroux, J.P. Basly, Inhibitory effect of curcuminoids on MCF-7 cell proliferation and structure-activity relationships, Cancer Lett. 129 (1998) 111–116.
[23] R. Adhikary, C.A. Barnes, R.L. Trampel, S.J. Wallace, Photoinduced *trans*-to-*cis* isomerization of cyclocurcumin, J. Phys. Chem. B 115 (2011) 10707–10714.
[24] R.A. Khera, R. Ahmad, I. Ullah, O.-U.-R. Abid, O. Fatunsia, M. Sher, A. Villinger, P. Langer, Cyclization vs. elimination reactiona of 5-aryl-5-hydroxy 1,3-diones one-pot synthesis of 2-aryl-2,3-dihydro-4*H*-pyran-4-ones, Helv. Chim. Acta 93 (2013) 1705–1715.
[25] S. Dorai, W. Shi, C. Corbo, C. Sun, S. Averick, "Clicked" sugar-curcumin conjugate: modulator of amyloid-β and tau peptide aggregation at ultralow concentrations, ACS Chem. Neurosci. 2 (2011) 694–699.
[26] C.A. Lipinski, F. Lombardo, B.W. Dominy, P.J. Feeney, Experimental and computational approaches to estimate solubility and permeability in drug discovery and development settings, Adv. Drug. Delivery Rev. 23 (1997) 3–25.
[27] K. Ono, K. Hasegawa, H. Naiki, M. Yamada, Curcumin has potent anti-amyloidogenic effects for Alzheimer's beta-amyloid fibrils in vitro, J. Neuro Research. 75 (2004) 742–750.
[28] (a) A.L. Cheng, C.H. Hsu, J.K. Lin, M.M. Hsu, Y.F. Ho, T.S. Shen, J.Y. Ko, J.Y. Lin, B. R. Lin, W. Ming-Shiang, H.S. Yu, S.H. Jee, G.S. Chen, T.M. Chen, C.A. Chen, M.K. Lai, Y.S. Pu, M.H. Pan, Y.J. Wang, C.C. Tsai, C.Y. Hsieh, Phase I clinical trial of curcumin, a chemopreventive agent, in patients with high-risk or pre-malignant lesions, Anticancer research 21 (2001) 2895-2900. (b) B. Jiang, A. Aliyan, N.P. Cook, A. Augustine, G. Bhak, R. Maldonado, A.D.S. McWilliams, E.M. Flores, N. Meddez, M. Shahnawaz, F.J. Godoy, J. Montenegro, I. Moreno-Gonzelez, A.A. Marti, Monitoring the formation of amyloid oligomaers using photoluminescence anisotropy, J. Am. Chem. Soc. 141 (2019) 15605-15610.
[29] The software was prepared by the Cambridge Crystallographic Data Centre (CCDC). http://www.ccdc.cam.ac.uk.